



Cite this: *Polym. Chem.*, 2015, **6**, 827

# Precision synthesis of macrocyclic giant surfactants tethered with two different polyhedral oligomeric silsesquioxanes at distinct ring locations *via* four consecutive “click” reactions†

Yiwen Li,<sup>‡a</sup> Hao Su,<sup>‡a</sup> Xueyan Feng,<sup>‡a</sup> Kan Yue,<sup>a</sup> Zhao Wang,<sup>a</sup> Zhiwei Lin,<sup>a</sup> Xiulin Zhu,<sup>b</sup> Qiang Fu,<sup>c</sup> Zhengbiao Zhang,<sup>\*b</sup> Stephen Z. D. Cheng<sup>\*a</sup> and Wen-Bin Zhang<sup>\*a,d</sup>

The combined utilization of chemoselective “click” chemistry allows for the preparation of well-defined macromolecules with complex compositions and architectures. In this article, we employed the sequential “click” strategy to further expand the scope of synthetically available giant molecules by precisely constructing new giant surfactants based on polyhedral oligomeric silsesquioxane (POSS) tethered cyclic polymers. The general synthetic approach involves sequentially performed strain-promoted azide–alkyne cycloaddition (SPAAC) as a method for bimolecular homobifunctional ring closure, copper-catalyzed azide–alkyne cycloaddition (CuAAC) for POSS–polymer conjugation, and thiol–Michael/thiol–ene reactions for POSS surface functionalization. Specifically, a cyclic polymer tethered with two POSS cages of distinct surface chemistry at different locations of the chain has been prepared. This work promises to afford numerous cyclic polymers-based giant surfactants with diverse structural variations for further investigation on unexpected physical properties.

Received 4th October 2014,  
Accepted 27th October 2014

DOI: 10.1039/c4py01360c

www.rsc.org/polymers

## Introduction

The sophisticated use of advanced functional soft materials possessing well-defined chemical functionalities and desired physical properties may hold the key to the development of nanoscience and nanotechnology.<sup>1,2</sup> It is anticipated that achieving structural precision in macromolecules could lead to desired materials with finely tunable functions and pro-

perties.<sup>3</sup> Extensive efforts have been devoted to the exact control over the molecular architectures and functionalities in polymeric materials, which usually take advantage of unparalleled accuracy in molecular-level structural control using organic chemistry, allowing the design and synthesis of precisely-defined macromolecules.<sup>3</sup>

“Click” chemistry serves as a powerful strategy in the quest for “precision synthesis” in polymer chemistry since it offers a family of selective and orthogonal reactions with high efficiency under mild conditions.<sup>4–7</sup> So far, different kinds of chemical ligations, such as Cu(I)-catalyzed [3 + 2] azide–alkyne cycloaddition (CuAAC),<sup>8–10</sup> strain-promoted azide–alkyne cycloaddition (SPAAC),<sup>11</sup> Diels–Alder cycloaddition,<sup>12,13</sup> thiol–ene reaction,<sup>14–17</sup> and oxime ligation,<sup>18</sup> exhibit several features of an ideal “click” reaction. Specifically, the combined utilization of multiple “click” reactions provides numerous opportunities to engineer multifunctional and tunable macromolecular materials without sacrificing the synthetic simplicity and efficiency,<sup>2,19</sup> and these classes of materials possess a broad range of applications from microelectronics<sup>2</sup> to nanomedicine.<sup>20</sup>

As a new class of amphiphiles that bridge the gap between small-molecule surfactants and block copolymers, giant surfactants have received increasing attentions in the recent years because of their unique structural features similar to small-molecule surfactants with size amplification and attractive

<sup>a</sup>Department of Polymer Science, College of Polymer Science and Polymer Engineering, The University of Akron, Akron, Ohio 44325–3909, U.S.A.

E-mail: scheng@uakron.edu; Fax: +1 330 972 8626; Tel: +1 330 972 6931

<sup>b</sup>Jiangsu Key Laboratory of Advanced Functional Polymer Design and Application, Department of Polymer Science and Engineering, College of Chemistry, Chemical Engineering and Materials Science, Soochow University, Suzhou 215123, P. R. China. E-mail: zhangzhengbiao@suda.edu.cn; Fax: +86-512-65112796;

Tel: +86-512-65880819

<sup>c</sup>College of Polymer Science & Engineering, State Key Laboratory of Polymer Materials Engineering, Sichuan University, Chengdu 610065, China

<sup>d</sup>Key Laboratory of Polymer Chemistry & Physics of Ministry of Education, College of Chemistry and Molecular Engineering, Center for Soft Matter Science and Engineering, Peking University, Beijing 100871, China. E-mail: wenbin@pku.edu.cn; Fax: +86 10 6275 1708; Tel: +86 10 6275 2394

†Electronic supplementary information (ESI) available: Details of characterization data including the synthesis and characterization of the compounds. See DOI: 10.1039/c4py01360c

‡These authors contributed equally to this work.

dual properties in their self-assembly behaviors in the bulk and in solution.<sup>21–24</sup> Giant surfactants are a subclass of giant molecules and usually refer to polymer-tethered molecular nanoparticles in general.<sup>21</sup> Recently, significant progress has been made in the development of precisely-defined giant surfactants with a large variety of chemical compositions and macromolecular architectures by introducing polyhedral oligomeric silsesquioxane (POSS)<sup>25–31</sup> as the head group. The self-organization of POSS-based giant surfactants are able to present a promising way to generate several types of hierarchical structures with sub-10 nm feature sizes.<sup>22</sup> More interestingly, it was found that the increase of macromolecular structural complexity of giant surfactants enables the formation of various unprecedented supramolecular hierarchical structures, which may result in unique physical properties.<sup>21</sup> Therefore, the current resurgence of interest in giant molecules benefits from the rapid and precise preparation of new giant surfactants with diverse structural variations for further generating a dynamic, exciting and interdisciplinary research field.<sup>21,24</sup>

Cyclic polymers represent an important class of non-linear topological macromolecules with no chain ends.<sup>32–35</sup> Due to their unique topology, they usually exhibit intriguing physical properties such as decreased glass transition temperatures and viscosity,<sup>35</sup> and biological activities for example enhanced targeting efficiency<sup>36</sup> and increased circulation time in bloodstream.<sup>37</sup> Additionally, applications of highly efficient and orthogonal coupling approaches such as “click” chemistry promise to improve the availability of a wide-range of well-defined cyclic macromolecule-based hybrid materials with tailored architectures and functions.<sup>32,38–42</sup> It has also recently been demonstrated that cyclic protein or tadpole protein can be synthesized in cells *in situ* by highly reactive genetically encoded chemistry with improved stability.<sup>41,43</sup> While the integration of cyclic polymer with other topological macromolecules has been explored in depth, only a few examples of macrocycle–nanoparticle conjugates are known.<sup>44</sup> Considering that introducing macrocyclic segment into giant molecules could greatly increase the structural complexity of whole macromolecules, it is thus highly desirable to construct a series of cyclic polymer-based giant surfactants for further study on their structure–property relationships.

The “click” synthetic strategy *via* the combination of multiple orthogonal “click” reactions in either sequential or one-pot fashion has been pronounced in the precision synthesis of various multifunctional macromolecules.<sup>45,46</sup> Encouraged by the unparalleled efficiency and versatility of this general methodology, we strive to further extend the established approaches to the synthesis of macrocycle-based giant surfactants. Our new strategy involves sequentially performed SPAAC as a method for bimolecular homobifunctional ring closure, CuAAC for POSS–polymer conjugation, and thiol–Michael/thiol–ene reactions for POSS surface functionalization, which fully benefits from different chemical reactivity between cyclooctyne and terminal alkyne in the absence of Cu(I),<sup>47</sup> and between activated enes with vinyl siloxanes without radical

initiators.<sup>48</sup> As selected examples, two kinds of new giant surfactants containing functional POSS(s) as the head(s) tethered with macrocyclic polymer have been successfully prepared by using above strategy. Specifically, metal-free SPAAC was found to be another useful “click” method to prepare cyclic polymers, offering numerous opportunities for macromolecular cyclizations of biomacromolecules or polyelectrolytes in the future. This work offers a modular and facile access to giant molecules based on POSS–cyclic polymer conjugates with complex macromolecular architectures and novel compositions, which could also be easily extended to a wide range of other complex polymeric systems in general.

## Experimental section

### Chemicals and solvents

Styrene (Aldrich, 99%) was purified by distillation from calcium hydride under reduced pressure prior to use. Tetrahydrofuran (THF, Certified ACS, EM Science), methanol (Fisher Scientific, reagent grade), ethyl acetate (EtOAc, Fisher Scientific), toluene (Certified ACS), dichloromethane (Certified ACS), chloroform (Certified ACS), *N,N*-dimethylformamide (DMF, Aldrich, anhydrous 99.8%) and hexanes (Certified ACS) were used after distillation. Cuprous bromide (CuBr, Aldrich, 98%) was freshly purified by stirring in acetic acid overnight, washed with acetone, and dried in vacuum. 2-Mercaptoacetic acid (Aldrich, >98%) was distilled under reduced pressure before use. Octavinyl POSS (Hybrid Plastics, >97%), Acrylo POSS cage mixture (Hybrid Plastics, cage content >90%), *N,N,N',N',N''*-pentamethyldiethylenetriamine (PMDETA, Aldrich, 99%), 2-bromoisobutyl bromide (Aldrich, 98%), 1*H*,1*H*,2*H*,2*H*-perfluoro-1-decanethiol (Aldrich, 97%), hexylamine (Aldrich, 99%), 2,2-dimethoxy-2-phenylacetophenone (DMPA, Acros Organics, 99%), 1-thioglycerol (Sigma, >99%), *N,N'*-diisopropylcarbodiimide (DIPC, Acros Organics, 99%), 4-(dimethylamino)pyridine (Aldrich, 99%), sodium azide (Aldrich, >99%), succinic anhydride (Aldrich, >99%), *p*-toluenesulfonic acid (TsOH, Aldrich, 98.5%) were used as received. Silica gel (VWR, 230–400 mesh) was activated by heating to 140 °C for 12 h. Ultraviolet (UV) light irradiation of the samples was carried out with a 15 W UVP Black Ray UV bench lamp XX-15 L, emitting light with a wavelength of ~365 nm (intensity *ca.* 4.6 mW cm<sup>−2</sup>). 4-(Dimethylamino)pyridinium toluene-*p*-sulfonate (DPTS),<sup>9</sup> N<sub>3</sub>–PS–N<sub>3</sub>,<sup>49</sup> Alkyne–(PS–N<sub>3</sub>)<sub>2</sub>,<sup>50</sup> ACPOSS–COOH,<sup>51</sup> HO–(VPOSS)–OH,<sup>52</sup> DIBO–COOH<sup>46</sup> and DIBO–PEG<sub>6000</sub><sup>53</sup> were synthesized as reported, respectively.

### Characterization

Size exclusion chromatographic analyses (SEC) for the synthesized polymers were performed using a Waters 150-C Plus instrument equipped with three HR–Styragel columns [100 Å, mixed bed (50/500/10<sup>3</sup>/10<sup>4</sup> Å), mixed bed (10<sup>3</sup>, 10<sup>4</sup>, 10<sup>6</sup> Å)], and a triple detector system. The three detectors included a differential refractometer (Waters 410), a differential viscometer (Viscotek 100), and a laser light scattering detector (Wyatt Technology,

DAWN EOS,  $\lambda = 670$  nm). THF was used as eluent with a flow rate of  $1.0 \text{ mL min}^{-1}$  at  $30^\circ\text{C}$ .

All  $^1\text{H}$  and  $^{13}\text{C}$  NMR spectra were acquired in  $\text{CDCl}_3$  (Aldrich, 99.8% D) utilizing a Varian Mercury 300 NMR and 500 NMR spectrometer. The  $^1\text{H}$  NMR spectra were referenced to the residual proton signals in the  $\text{CDCl}_3$  at  $\delta$  7.27 ppm; while the  $^{13}\text{C}$  NMR spectra were referenced to  $^{13}\text{CDCl}_3$  at  $\delta$  77.00 ppm.

Infrared spectra were obtained on an Excalibur Series FT-IR spectrometer (DIGILAB, Randolph, MA) by casting films on KBr plates from solutions with subsequent drying at  $40$ – $50^\circ\text{C}$ . The spectroscopic data were processed using Win-IR software.

UV-Vis absorption spectra were collected using a Shimadzu 1750 UV-Vis spectrometer. The test sample was dissolved in chloroform at a concentration of  $50 \mu\text{mol mL}^{-1}$  and transferred to a quartz cuvette for measurement.

Matrix-assisted laser desorption/ionization time-of-flight (MALDI-TOF) mass spectra were acquired on a Bruker Ultraflex-III TOF/TOF mass spectrometer (Bruker Daltonics, Inc., Billerica, MA) equipped with a Nd:YAG laser ( $355 \text{ nm}$ ). All of the spectra were measured in positive reflection or linear mode. The instrument was calibrated prior to each measurement with external PMMA or PS standards at the molecular weight under consideration. The compound *trans*-2-[3-(4-*tert*-butylphenyl)-2-methyl-2-propenylidene]-malononitrile (DCTB, Aldrich, >98%) served as matrix and was prepared in  $\text{CHCl}_3$  at a concentration of  $20 \text{ mg mL}^{-1}$ . The cationizing agent sodium trifluoroacetate or silver trifluoroacetate was prepared in  $\text{MeOH-CHCl}_3$  ( $v/v = 1/3$ ) at a concentration of  $5 \text{ mg mL}^{-1}$  or  $10 \text{ mg mL}^{-1}$ . The matrix and cationizing salt solutions were mixed in a ratio of 10/1 ( $v/v$ ). All samples were dissolved in  $\text{CHCl}_3$  at a concentration of  $10 \text{ mg mL}^{-1}$ . The sample preparation followed the procedure of depositing  $0.5 \mu\text{L}$  of matrix and salt mixture on the wells of a 384-well ground-steel plate, allowing the spots to dry, depositing  $0.5 \mu\text{L}$  of each sample on a spot of dry matrix/salt, and adding another  $0.5 \mu\text{L}$  of matrix and salt mixture on top of the dry sample (sandwich method). After solvent evaporation, the plate was inserted into the MALDI mass spectrometer. The attenuation of the Nd:YAG laser was adjusted to minimize undesired polymer fragmentation and to maximize the sensitivity.

Thin-layer chromatographic analyses of the functionalized polymers were carried out by spotting samples on flexible silica gel plates (Selecto Scientific, Silica Gel 60, F-254 with fluorescent indicator) and developing using toluene or its mixture with other polar solvents.

## Synthetic procedures

**DIBO-(VPOSS)-DIBO.** To a  $100 \text{ mL}$  round-bottomed flask equipped with a magnetic stirring bar was added HO-(VPOSS)-OH ( $741 \text{ mg}$ ,  $1.0 \text{ mmol}$ ), DIBO-COOH ( $674 \text{ mg}$ ,  $2.1 \text{ mmol}$ ) and DPTS ( $620 \text{ mg}$ ,  $2.1 \text{ mmol}$ ), followed by the addition of  $35 \text{ mL}$  freshly dried DMF to fully dissolve the solids. The mixture was capped by a rubber septum, cooled to  $0^\circ\text{C}$  and stirred for  $10 \text{ min}$  before DIPC ( $378 \text{ mg}$ ,  $3.0 \text{ mmol}$ ) was added dropwise *via* a syringe. The mixture was allowed to warm up to room

temperature and stirred for another  $12 \text{ hours}$ . The white precipitates were then filtered off and the filtrate was washed with water and brine, dried over  $\text{Na}_2\text{SO}_4$ . After solvent removal, the residue was purified by flash chromatography on silica gel using  $\text{CH}_2\text{Cl}_2$  as the eluent to afford the product as a white powder ( $1144 \text{ mg}$ ,  $85\%$ ).  $^1\text{H}$  NMR ( $300 \text{ MHz}$ ,  $\text{CDCl}_3$ , ppm,  $\delta$ ):  $7.54$  (m,  $2\text{H}$ , aromatic),  $7.40$ – $7.27$  (m,  $14\text{H}$ , aromatics),  $6.15$ – $5.85$  (m,  $21\text{H}$ ,  $-\text{CH}=\text{CH}_2$ ),  $5.59$  (s,  $1\text{H}$ ,  $-\text{CHOCO}-$ ),  $5.18$  (m,  $1\text{H}$ ,  $-\text{SCH}_2\text{CH}-$ ),  $4.40$  (m,  $1\text{H}$ ,  $-\text{CH}_2\text{OCO}-$ ),  $4.25$  (m,  $1\text{H}$ ,  $-\text{CH}_2\text{OCO}-$ ),  $3.18$  (dd,  $1\text{H}$ ,  $-\text{CH}_2\text{CHOCO}-$ ),  $2.95$  (dd,  $1\text{H}$ ,  $-\text{CH}_2\text{CHOCO}-$ ),  $2.83$ – $2.58$  (m,  $12\text{H}$ ,  $-\text{CH}_2\text{SCH}_2-$  +  $-\text{OCC}_2\text{H}_4\text{COO}-$ ),  $1.08$  (t,  $2\text{H}$ ,  $-\text{SiCH}_2-$ ).  $^{13}\text{C}$  NMR ( $75 \text{ MHz}$ ,  $\text{CDCl}_3$ , ppm,  $\delta$ ):  $172.08$ ,  $171.07$ ,  $151.07$ ,  $137.34$ ,  $130.17$ ,  $128.76$ ,  $128.31$ ,  $127.45$ ,  $126.45$ ,  $126.11$ ,  $123.85$ ,  $121.51$ ,  $113.16$ ,  $109.99$ ,  $71.02$ ,  $64.20$ ,  $46.46$ ,  $32.04$ ,  $29.33$ ,  $26.93$ ,  $13.22$ . MS (MALDI-TOF): Calcd for  $\text{C}_{59}\text{H}_{60}\text{NaO}_{20}\text{SSi}_8$   $1367.15$ , found:  $1367.48$  ( $\text{M}^+\text{Na}^+$ ).

**ACPOSS- $\text{N}_3$ .** To a  $100 \text{ mL}$  round-bottomed flask equipped with a magnetic stirring bar was added ACPOSS-COOH ( $300 \text{ mg}$ ,  $0.212 \text{ mmol}$ ),  $\text{HO-N}_3$  ( $52 \text{ mg}$ ,  $0.233 \text{ mmol}$ ) and DPTS ( $63 \text{ mg}$ ,  $0.212 \text{ mmol}$ ), followed by the addition of  $20 \text{ mL}$  freshly dried  $\text{CH}_2\text{Cl}_2$  to fully dissolve the solids. The mixture was capped by a rubber septum, cooled to  $0^\circ\text{C}$  and stirred at that temperature for  $10 \text{ min}$ , and then DIPC ( $40 \text{ mg}$ ,  $0.318 \text{ mmol}$ ) was added dropwise *via* syringe. The mixture was allowed to warm up to room temperature and stirred for another  $12 \text{ h}$ . The white precipitation was then filtered off and the filtrate was washed with water and brine, dried over  $\text{Na}_2\text{SO}_4$ . After solvent removal, the residue was purified by flash chromatography on silica gel with  $\text{CH}_2\text{Cl}_2$ -EtOAc ( $v/v = 20/3$ ) as the eluent to afford the product ( $245 \text{ mg}$ ,  $72\%$ ).  $^1\text{H}$  NMR ( $500 \text{ MHz}$ ,  $\text{CDCl}_3$ , ppm,  $\delta$ ):  $8.05$  (d,  $2\text{H}$ ,  $-\text{OCC}_2\text{H}_2-$ ),  $7.39$  (d,  $2\text{H}$ ,  $-\text{CH}_2\text{CC}_2\text{H}_2-$ ),  $6.37$  (d,  $7\text{H}$ ,  $\text{CH}_a\text{H}_b=\text{CH}-$ ),  $6.13$  (q,  $7\text{H}$ ,  $\text{CH}_a\text{H}_b=\text{CH}-$ ),  $5.82$  (d,  $7\text{H}$ ,  $\text{CH}_a\text{H}_b=\text{CH}-$ ),  $4.47$  (m,  $4\text{H}$ ,  $-\text{OC}_2\text{H}_4\text{O}-$ ),  $4.13$  (m,  $18\text{H}$ ,  $-\text{CH}_2\text{OCO}-$  +  $-\text{CH}_2\text{N}_3$ ),  $3.29$  (s,  $2\text{H}$ ,  $-\text{SCH}_2\text{COO}-$ ),  $2.90$  (t,  $2\text{H}$ ,  $-\text{CH}_2\text{SCH}_2\text{COO}-$ ),  $2.62$  (t,  $2\text{H}$ ,  $-\text{CH}_2\text{CH}_2\text{S}-$ ),  $1.77$  (m,  $16\text{H}$ ,  $-\text{SiCH}_2\text{CH}_2-$ ),  $0.71$  (t,  $16\text{H}$ ,  $-\text{SiCH}_2-$ ).  $^{13}\text{C}$  NMR ( $75 \text{ MHz}$ ,  $\text{CDCl}_3$ , ppm,  $\delta$ ):  $171.47$ ,  $170.08$ ,  $166.11$ ,  $130.53$ ,  $130.25$ ,  $128.51$ ,  $127.97$ ,  $66.12$ ,  $62.98$ ,  $62.61$ ,  $54.26$ ,  $34.16$ ,  $33.46$ ,  $29.67$ ,  $27.53$ ,  $22.13$ ,  $8.03$ . MS (MALDI-TOF): Calcd for  $\text{C}_{60}\text{H}_{85}\text{N}_3\text{NaO}_{32}\text{SSi}_8$   $1638.29$ , found:  $1638.47$  ( $\text{M}^+\text{Na}^+$ ).

**VPOSS-cPS.** To a  $500 \text{ mL}$  uncapped beaker equipped with a magnetic stirring bar was added DIBO-(VPOSS)-DIBO ( $100 \text{ mg}$ ,  $0.074 \text{ mmol}$ ) dissolved in  $300 \text{ mL}$  THF solution, followed by the slow addition of  $100 \text{ mL}$  THF solution of  $\text{N}_3\text{-PS-N}_3$  ( $M_n = 4.4 \text{ kg mol}^{-1}$ , PDI =  $1.04$ ,  $344 \text{ mg}$ ,  $0.078 \text{ mmol}$ ). This reaction was monitored by UV-Vis spectrometry. After stirring for about  $2 \text{ days}$ , there was no detectable absorbance for DIBO ( $306 \text{ nm}$ ). The solution was then concentrated in about  $5 \text{ mL}$  by evaporating the excess solvent. Excess DIBO-PEG<sub>6000</sub> ( $50 \text{ mg}$ ) was further added into the concentrated solution to react with all azido-terminated materials about  $2 \text{ hours}$ . After complete reaction, the solution was directly transferred onto the top of a silica gel column. A mixture of  $\text{CHCl}_3$  and EtOAc ( $v/v = 1/20$ ) was used to elute the product off the column. After solvent removal, the crude product was precipitated into cold MeOH.

After filtration, the sample VPOSS-cPS was collected and dried under vacuum overnight to give a white powder (219 mg; Yield: 51%). NMR:  $M_{n, \text{NMR}} = 5.8 \text{ kg mol}^{-1}$ ; SEC:  $M_{n, \text{SEC}} = 5.0 \text{ kg mol}^{-1}$ , PDI = 1.03.

**APOSS-cPS.** VPOSS-cPS ( $M_{n, \text{NMR}} = 5.8 \text{ kg mol}^{-1}$ , 200 mg, 34.5  $\mu\text{mol}$ ), 2-mercaptoacetic acid (64 mg, 690  $\mu\text{mol}$ ), and DMPA (2 mg, 5  $\mu\text{mol}$ ) were dissolved in 5 mL of THF, followed by irradiation with UV 365 nm for 30 minutes. The solution was then precipitated into cold methanol three times. The sample APOSS-cPS was collected and dried under vacuum overnight to afford a white powder (167 mg; Yield: 77%). NMR:  $M_{n, \text{NMR}} = 6.3 \text{ kg mol}^{-1}$ ; SEC:  $M_{n, \text{SEC}} = 4.7 \text{ kg mol}^{-1}$ , PDI = 1.07.

**VPOSS-cPS-alkyne.** To a 500 mL uncapped beaker equipped with a magnetic stirring bar was added DIBO-(VPOSS)-DIBO (100 mg, 0.074 mmol) dissolved in 300 mL THF solution, followed by the slow addition of 100 mL THF solution of Alkyne-(PS- $\text{N}_3$ )<sub>2</sub> ( $M_n = 3.3 \text{ kg mol}^{-1}$ , PDI = 1.06, 257 mg, 0.078 mmol). This reaction was monitored by UV-Vis spectrometry. After stirring for about 2 days, there was no detectable absorbance for DIBO (306 nm). The solution was then concentrated in about 5 mL by evaporating the excess solvent. DIBO-PEG<sub>6000</sub> was further added into the concentrated solution to react with all azido-terminated materials about 2 hours. After complete reaction, the solution was directly transferred onto the top of a silica gel column. A mixture of  $\text{CHCl}_3$  and EtOAc ( $v/v = 1/20$ ) was used to elute the product off the column. After solvent removal, the crude product was precipitated into cold MeOH. After filtration, the sample VPOSS-cPS-alkyne was collected and dried under vacuum overnight to give a white powder (167 mg; Yield: 48%). NMR:  $M_{n, \text{NMR}} = 4.7 \text{ kg mol}^{-1}$ ; SEC:  $M_{n, \text{SEC}} = 3.8 \text{ kg mol}^{-1}$ , PDI = 1.02.

**VPOSS-cPS-ACPOSS.** To a 100 mL Schlenk flask equipped with a magnetic stirring bar was added VPOSS-cPS-alkyne ( $M_{n, \text{NMR}} = 4.7 \text{ kg mol}^{-1}$ , 200 mg, 42.6  $\mu\text{mol}$ ), fresh prepared ACPOSS- $\text{N}_3$  (72 mg, 44.7  $\mu\text{mol}$ ), CuBr (1 mg, 5  $\mu\text{mol}$ ), and freshly distilled toluene (10 mL). The resulting solution was degassed by three freeze-pump-thaw cycles before the addition of PMDETA (20 mg, 0.113 mmol) *via* a pipet. The mixture was further degassed by one freeze-pump-thaw cycle, and was then stirred at room temperature for 24 hours. After complete reaction, the solution was directly transferred onto the top of a silica gel column. Then a mixture of  $\text{CHCl}_3$  and EtOAc ( $v/v = 2/20$ ) was used to elute the product off the column. After solvent removal, the crude product was precipitated into cold methanol. After filtration, the sample VPOSS-cPS-ACPOSS was collected and dried under vacuum overnight to give a white powder (207 mg; Yield: 76%). NMR:  $M_{n, \text{NMR}} = 6.4 \text{ kg mol}^{-1}$ ; SEC:  $M_{n, \text{SEC}} = 5.8 \text{ kg mol}^{-1}$ , PDI = 1.05.

**VPOSS-cPS-FPOSS.** VPOSS-cPS-ACPOSS ( $M_{n, \text{NMR}} = 6.4 \text{ kg mol}^{-1}$ , 100 mg, 15.6  $\mu\text{mol}$ ), 1*H*,1*H*,2*H*,2*H*-perfluoro-1-decanethiol (150 mg, 312  $\mu\text{mol}$ ), and hexylamine (1 mg) were added to an open vial equipped a magnetic stirring bar and dissolved in 5 mL THF. The solution was stirred at room temperature for about 1 hour. The mixture was then precipitated into a cold mixture of methanol-hexanes ( $v/v = 5/1$ ) three times. The product was collected and dried under vacuum overnight to

afford a white powder (127 mg; Yield: 85%). NMR:  $M_{n, \text{NMR}} = 9.6 \text{ kg mol}^{-1}$ ; SEC:  $M_{n, \text{SEC}} = 8.7 \text{ kg mol}^{-1}$ , PDI = 1.04.

**APOSS-cPS-FPOSS.** VPOSS-cPS-FPOSS ( $M_{n, \text{NMR}} = 9.6 \text{ kg mol}^{-1}$ , 100 mg, 10.4  $\mu\text{mol}$ ), 2-mercaptoacetic acid (19 mg, 208  $\mu\text{mol}$ ), and DMPA (1 mg) were dissolved in 5 mL of THF, followed by irradiation with UV 365 nm for 30 minutes. The solution was then precipitated into cold methanol three times. The product was collected and dried under vacuum overnight to afford a white powder (84 mg; Yield: 82%). NMR:  $M_{n, \text{NMR}} = 9.9 \text{ kg mol}^{-1}$ ; SEC:  $M_{n, \text{SEC}} = 8.0 \text{ kg mol}^{-1}$ , PDI = 1.07.

## Results and discussion

### POSS-based “clickable” building blocks with two cyclooctynes

SPAAC between cyclooctynes and azides has emerged as a bio-orthogonal, metal-free, and highly efficient chemical ligation tool for POSS-polymer conjugates,<sup>46,54</sup> especially when biomacromolecules or polyelectrolytes are involved.<sup>55</sup> Considering its excellent performance in bioconjugation in extremely dilute solutions and high tolerance to a wide range of experimental conditions,<sup>55</sup> SPAAC seems to be an ideal tool for macromolecular cyclization although few related work were documented before. To address this issue, a POSS-based “click” building block possessing strained alkynes is a prerequisite. This can be simply achieved by the esterification between an established POSS diol, HO-(VPOSS)-OH,<sup>56</sup> and cyclooctyne acid, DIBO-COOH.<sup>46</sup> It was performed with a stoichiometric mixture of both chemicals in the presence of 4-(dimethylamino) pyridinium toluene-*p*-sulfonate (DPTS) and *N,N'*-diisopropylcarbodiimide (DIPC) in dry DMF. The product, DIBO-(VPOSS)-DIBO, was purified by flash chromatography as a white solid in a good yield (85%). The introduction of DIBO moieties was evident by the appearance of characteristic resonances of aromatic protons at  $\delta$  7.54–7.27 ppm in <sup>1</sup>H NMR spectrum (Fig. 1a) and related new peaks for aromatic carbons from  $\delta$  130.17 to 121.51 ppm in <sup>13</sup>C NMR spectrum (Fig. S1a†). Additionally, the observation of a strong UV absorbance peak at  $\sim$ 306 nm that is characteristic of DIBO group in UV-Vis spectrum (Fig. S2a†) also supports the conclusion of successful reaction.<sup>47</sup> The molecular structure and purity of DIBO-(VPOSS)-DIBO are further confirmed by the MALDI-TOF mass spectrum where only one single peak matching with the mass of the proposed structures is found. The mass peak at  $m/z$  1367.48 shown in Fig. 2a perfectly agrees with the calculated monoisotopic molecular mass for the desired product (C<sub>59</sub>H<sub>60</sub>NaO<sub>20</sub>SSi<sub>8</sub> 1367.15 Da). The presence of two DIBO units on each POSS cage allows the bimolecular cyclization with a homobifunctional  $\alpha$ ,  $\omega$ -diazidopolymer to construct the macromolecular precursor based on VPOSS-tethered cyclic polymers. The vinyl groups on the VPOSS head can be further converted into diverse surface functionalities as usual. Therefore, new giant surfactants based on macrocycles can be directly achieved by combining SPAAC and thiol-ene reaction in a sequential fashion. In addition, this general and robust methodology also enables the precision synthesis of related



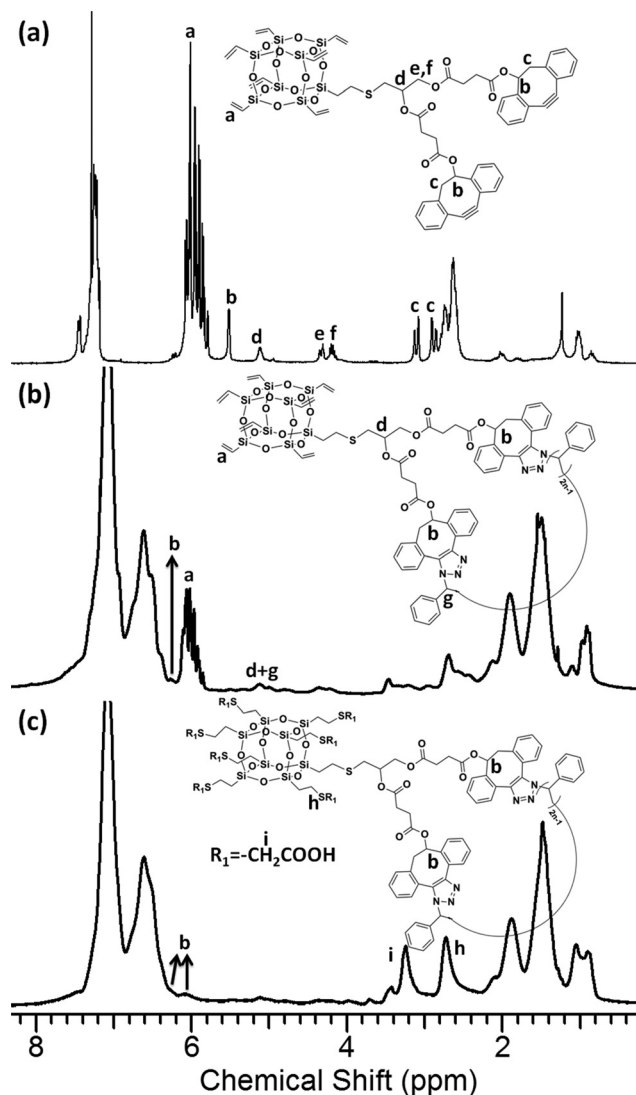


Fig. 1  $^1\text{H}$  NMR spectra of (a) DIBO-(VPOSS)-DIBO, (b) VPOSS-cPS, and (c) APOSS-cPS.

macromolecular derivatives with even more complex chemical compositions and molecular architectures by further introducing other “click” functionalities.

#### Giant surfactant based on POSS tethered macrocyclic polymer

The feasibility and efficiency of SPAAC for bimolecular homobifunctional cyclization was firstly examined by the model reaction between DIBO-(VPOSS)-DIBO and  $\text{N}_3\text{-PS-N}_3$  ( $M_n = 4.4 \text{ kg mol}^{-1}$ , PDI = 1.04) in dilute solution. The reaction was monitored by the absorbance intensity of DIBO group using UV-Vis spectrometry. It was completed in about 2 days until no UV absorbance at 306 nm can be observed (Fig. S2†). Note that the crude samples may include the desired product, unreacted  $\text{N}_3\text{-PS-N}_3$ , and some linear condensed byproducts. Since a slight excess of azido-polymers was used, the linear condensed byproducts are likely to possess azido groups at the polymer chain ends. Therefore, we were able to employ strained alkyne functionalized PEO to facilitate the removal of byproducts by chromatography. It ought to be expected that terminal alkyne functionalized resins should work as well for this system, as reported in literature.<sup>57</sup> The pure target product, VPOSS-cPS, was obtained as a white solid powder in a good yield (~50%) by precipitation into cold methanol.

Results obtained on various molecular characterizations including  $^1\text{H}$  NMR (Fig. 1),  $^{13}\text{C}$  NMR (Fig. S1†), UV-Vis (Fig. S2†), FT-IR (Fig. S3†), SEC (Fig. 3a) and MALDI-TOF mass spectrometry (Fig. 2b) fully support the successful preparation of a VPOSS cyclic PS conjugate. First, the “endless” feature of VPOSS-cPS is supported by the disappearance of both DIBO and azide groups. The former is evident by the missing DIBO absorption at 306 nm in the UV-Vis spectrum (Fig. S2†); while the latter can be directly proved by the observation of no characteristic vibrational band for the azido group at  $\sim 2100 \text{ cm}^{-1}$  in the FT-IR spectrum (Fig. S3†). Second, the intact VPOSS unit after the stoichiometric SPAAC cyclization process is confirmed by the resonant signals at  $\delta 6.19\text{--}5.94 \text{ ppm}$  in the  $^1\text{H}$  NMR spectrum (Fig. 1b) and  $\text{sp}^2$  carbon signals at  $\delta 137.16$  and  $128.65 \text{ ppm}$  in the  $^{13}\text{C}$  NMR spectrum (Fig. S1b†). Moreover, the SEC overlay (Fig. 3a) shows a single symmetric distribution for VPOSS-cPS ( $M_{n, \text{SEC}} = 5.0 \text{ kg mol}^{-1}$ , PDI = 1.03,

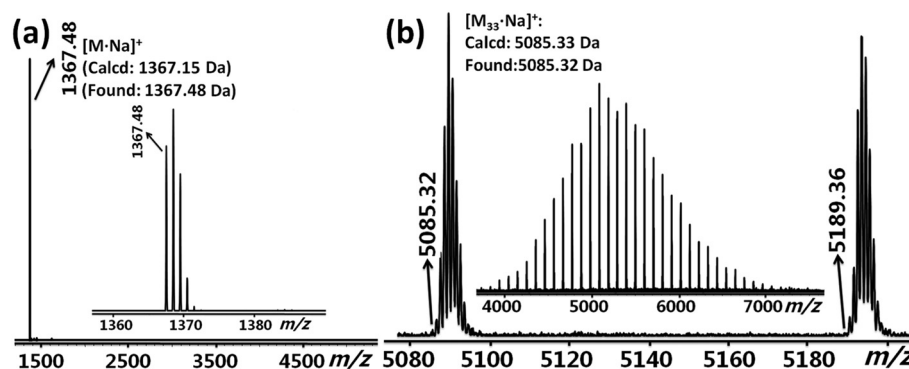


Fig. 2 MALDI-TOF mass spectra of (a) DIBO-(VPOSS)-DIBO, and (b) VPOSS-cPS. Both spectra were obtained in reflection mode with monoisotopic resolution. The insets show the corresponding full spectra.

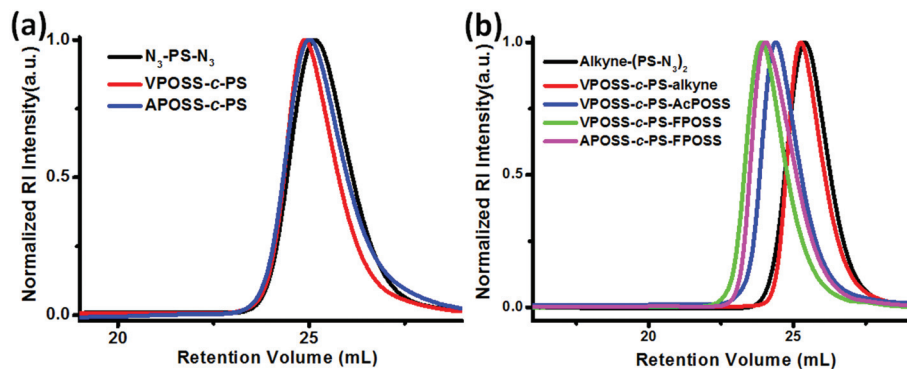


Fig. 3 SEC overlays for polymers: (a)  $N_3$ -PS- $N_3$  (black curve), VPOSS-c-PS (red curve), and APOSS-c-PS (blue curve); (b) Alkyne-(PS- $N_3$ )<sub>2</sub> (black curve), VPOSS-c-PS-alkyne (red curve), VPOSS-c-PS-ACPOSS (blue curve), VPOSS-c-PS-FPOSS (green curve), and APOSS-c-PS-FPOSS (magenta curve).

Table 1 Summary of molecular weight characterizations<sup>a</sup>

Sample	Molecular Formula <sup>a</sup>	$M$ (calcd) <sup>b</sup> (Da)	$m/z$ (obs.) <sup>c</sup>	$M_n$ , NMR (g mol <sup>-1</sup> )	$M_n$ , SEC (g mol <sup>-1</sup> )	PDI
VPOSS-cPS	C <sub>333</sub> H <sub>340</sub> N <sub>6</sub> NaO <sub>24</sub> SSi <sub>8</sub>	5085.33	5085.32	5.8 k	5.0 k	1.03
APOSS-cPS	—	—	—	6.3 k	4.7 k	1.07
VPOSS-cPS-alkyne	C <sub>291</sub> H <sub>298</sub> N <sub>6</sub> NaO <sub>26</sub> SSi <sub>8</sub>	4571.00	4571.38	4.7 k	3.8 k	1.02
VPOSS-cPS-ACPOSS	C <sub>335</sub> H <sub>367</sub> N <sub>9</sub> NaO <sub>58</sub> S <sub>2</sub> Si <sub>16</sub>	5978.17	5979.14	6.4 k	5.8 k	1.05
VPOSS-cPS-FPOSS	C <sub>429</sub> H <sub>426</sub> F <sub>119</sub> N <sub>9</sub> NaO <sub>58</sub> S <sub>9</sub> Si <sub>16</sub>	9657.75	9658.47	9.6 k	8.7 k	1.04
APOSS-cPS-FPOSS	—	—	—	9.9 k	8.0 k	1.07

<sup>a</sup> The molecular formula (a), the calculated monoisotopic or average molecular weights (b), and the experimentally observed  $m/z$  (c) are based on a 33-mer of VPOSS-cPS, a 27-mer of VPOSS-cPS-alkyne, a 25-mer of VPOSS-cPS-ACPOSS, and a 28-mer of VPOSS-cPS-FPOSS with a sodium cation.

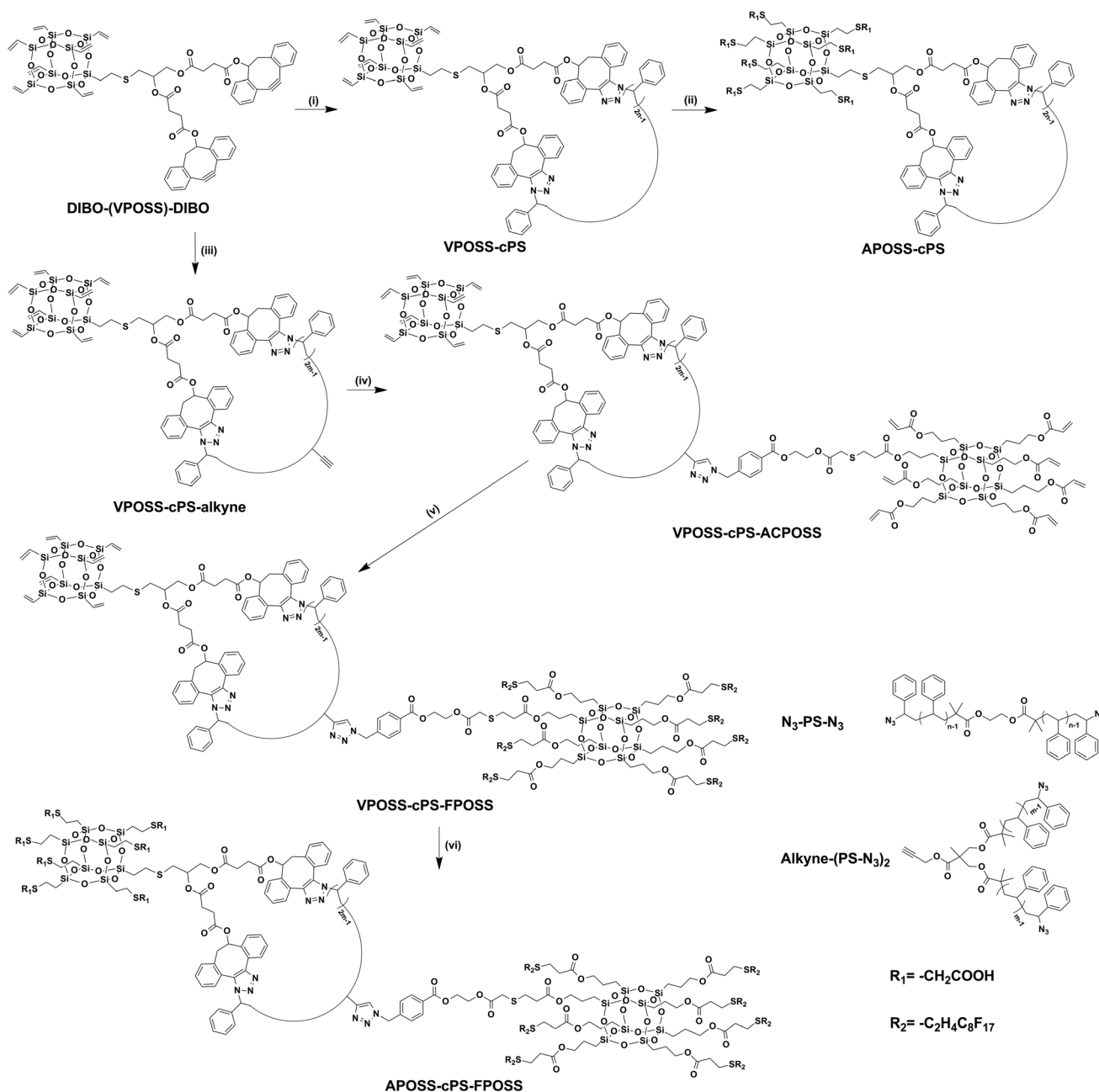
Table 1) shifted to a slightly lower retention volume relative to that of  $N_3$ -PS- $N_3$  ( $M_n = 4.4$  kg mol<sup>-1</sup>, PDI = 1.04) due to the balance between an increase in overall molecular weight (~1.3 kg mol<sup>-1</sup>) and a change in the hydrodynamic volume of cyclic polymer.<sup>39</sup> The most convincing evidence was obtained from the MALDI-TOF mass spectrum as shown in Fig. 2b. Only one single symmetric distribution of molecular weights was observed under the positive reflection mode, where the monoisotopic mass of each peak perfectly agrees with that expected for the proposed structure (e.g., for 33-mer with the formula of C<sub>333</sub>H<sub>340</sub>N<sub>6</sub>NaO<sub>24</sub>SSi<sub>8</sub>, observed  $m/z$  5085.32 Da vs. calcd 5085.32 Da). It is also clear from the spectrum that the mass difference between all adjacent two peaks is  $m/z$  104.04, exactly that of the styrene repeating unit. All of the above evidences confirm the macromolecular structure and purity of the desired product. Notably, due to the versatility and mild experimental conditions of SPAAC, this bimolecular homobifunctional cyclization should be easily extended to a wide range of synthetic and bio-polymers and block copolymers for fine-tuning cyclic compositions in giant surfactants.

The subsequent thiol-ene “click” chemistry provides a robust way for multi-site modification of VPOSS heads to introduce amphiphilicity of giant surfactants.<sup>58</sup> 2-Mercaptoacetic acid was thus used here to afford the model cyclic polymer-based giant surfactant, APOSS-cPS, under the typical radical-mediated thiol-ene reaction condition. After 30 min reaction, the disappearance of vinyl protons and unsaturated carbon resonances in the <sup>1</sup>H NMR (Fig. 1c) and <sup>13</sup>C NMR spectrum

(Fig. S1c†) validates the successful head “click” functionalization of VPOSS-cPS. Surprisingly, from the SEC overlay shown in Fig. 3a, it is found that the SEC trace of the final product, APOSS-cPS ( $M_n$ , SEC = 4.7 kg mol<sup>-1</sup>, PDI = 1.07), shifted to a larger retention volume compared with that of VPOSS-cPS, indicating that the introduction of amphiphilicity contributes more to the total hydrodynamic volume of cyclic polymer-based giant surfactant than the slight increase of the molecular weight.<sup>47</sup> All the above results unambiguously confirm the molecular structures and uniformity of the product, APOSS-cPS, which are expected to exhibit distinct self-assembling behaviors and generate unique hierarchical structures in comparison to their linear analogues due to more compact polymer structure of cyclic PS.<sup>40</sup>

#### Macrocylic giant surfactant tethered with two different POSSs at distinct ring locations

Cyclic polymer-based giant surfactants with more complex chemical compositions and molecular architectures can be further designed and synthesized in a modular fashion by incorporating other kinds of “click” chemistries,<sup>46</sup> such as CuAAC and thiol-Michael reaction.<sup>48</sup> Taking advantage of the distinctly different chemical reactivity between cyclooctyne and terminal alkyne in the absence of Cu(I),<sup>47</sup> and between activated enes with vinyl siloxanes without radical initiators,<sup>48</sup> we strive to extend the above established approach to facilitate a sequential multiple “click” strategy based on four kinds of “click” reactions (Scheme 1). This methodology was



**Scheme 1** Synthetic Route Using Multiple Sequential “click” Chemistry: (i) N<sub>3</sub>-PS-N<sub>3</sub>, THF, 25 °C, 51%; (ii) 2-mercaptoacetic acid, DMPA, *hν*, THF, 25 °C, 30 min, 77%; (iii) Alkyne-(PS-N<sub>3</sub>)<sub>2</sub>, THF, 25 °C, 48%; (iv) ACPOSS-N<sub>3</sub>, CuBr, PMDETA, toluene, 25 °C, 76%; (v) 1H,1H,2H,2H-perfluoro-1-decanethiol, hexylamine, THF, 25 °C, 1 h, 85%; (vi) 2-mercaptoacetic acid, DMPA, *hν*, THF, 25 °C, 30 min, 82%. (Note: SPAAC reaction generates two region-isomers and we only use 1,5-addition product to represent them for the sake of simplicity.)

demonstrated in a new giant surfactant system: a cyclic PS tethered with two different functional POSS heads at distinct ring locations.

The cyclic precursor, VPOSS-cPS-alkyne, was successfully prepared under exactly the same condition as SPAAC bimolecular homobifunctional cyclization for VPOSS-cPS described above, except that a PS with two terminal azido groups and a middle-chain alkyne group, Alkyne-(PS-N<sub>3</sub>)<sub>2</sub> (*M<sub>n</sub>* = 3.3 kg mol<sup>-1</sup>, PDI = 1.06), was used as the starting material. Similar to VPOSS-cPS, UV-vis (Fig. S4†) and FT-IR (Fig. S5†), results

confirm the complete consumption of DIBO and azido groups after SPAAC reaction by the disappearance of the corresponding peaks, respectively. The presence of VPOSS cage and pendant alkyne group was also proven by the corresponding signals in the NMR spectra. For example, the former is supported by the vinyl proton resonances at  $\delta$  6.14–5.86 ppm (Fig. 4a) and sp<sup>2</sup> carbons at  $\delta$  137.10 and 128.67 ppm (Fig. S6a†), while the latter one is revealed by the occurrence of proton (c) at  $\delta$  2.20 ppm in Fig. 4a and the carbon peak at  $\delta$  75.24 ppm in Fig. S6a.† In addition, the SEC diagram of

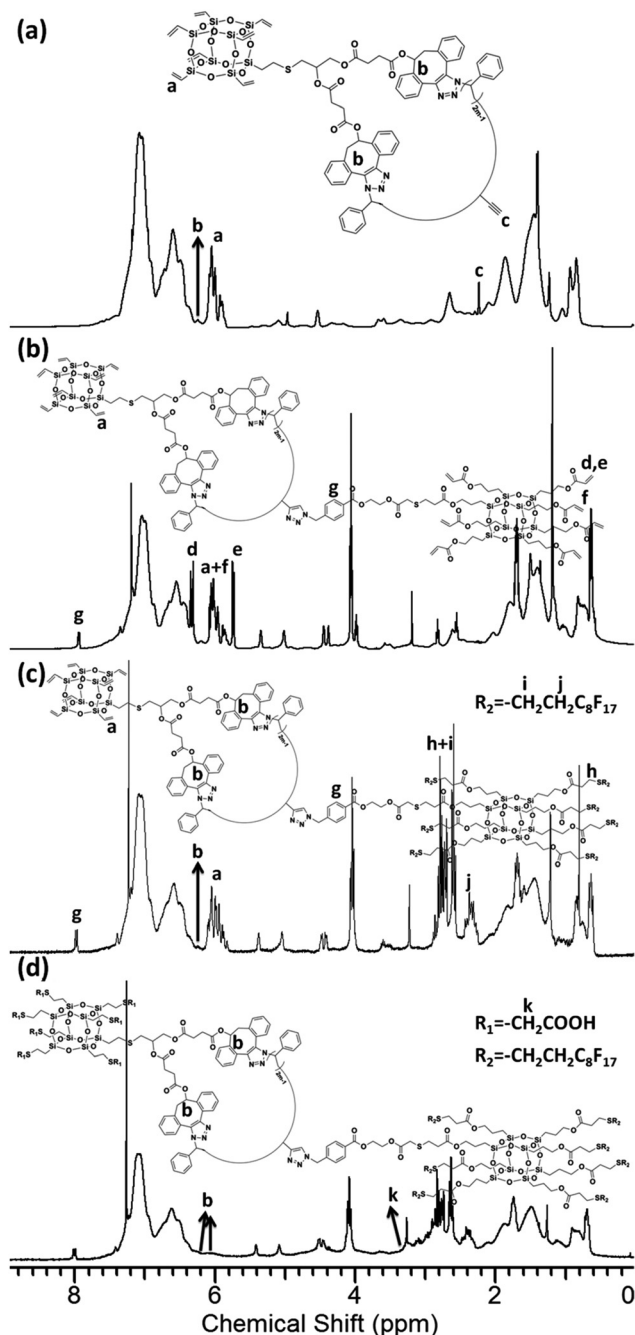


Fig. 4  $^1\text{H}$  NMR spectra of (a) VPOSS-cPS-alkyne, (b) VPOSS-cPS-ACPOSS, (c) VPOSS-cPS-FPOSS, and (d) APOSS-cPS-FPOSS.

VPOSS-cPS-alkyne ( $M_{n, \text{SEC}} = 3.8 \text{ kg mol}^{-1}$ , PDI = 1.02) (Fig. 3b) illustrates a mono-modal symmetric peak at only a slightly lower retention volume than that of Alkyne-(PS- $\text{N}_3$ )<sub>2</sub>, suggesting both molecular mass and the ring effect affect the overall hydrodynamic retention volume after cyclization. Moreover, the MALDI-TOF mass spectrum (Fig. 5a) shows only one single narrow distribution with molecular weights in accordance to the proposed structure. A representative monoisotopic mass peak at  $m/z$  4571.38 for VPOSS-cPS-alkyne ( $\text{Na}^+$  adduct) is in close match with the calculated molecular mass of 4571.00 Da

for 27-mer of the formula  $[\text{C}_{291}\text{H}_{298}\text{N}_6\text{NaO}_{26}\text{SSi}_8]^+$  (Fig. 5a & Table 1). All of the above evidence confirms the molecular structure of the desired product.

In Scheme 1, another type of POSS-based “clickable” building block with activated enes, was further tethered onto a defined position of PS macrocycle *via* CuAAC reaction between VPOSS-cPS-alkyne and freshly prepared ACPOSS- $\text{N}_3$  (Scheme S1†). The molecular structure and purity of the latter is supported by NMR techniques (Fig. S7a†) and MALDI-TOF mass spectrometry (Fig. S7b,† found 1638.47 Da *versus* calcd 1638.29 Da for  $(\text{M}\cdot\text{H})^+$ ). After the reaction, the successful installation of ACPOSS unit was revealed by the observation of new characteristic peaks for acryloyl group at  $\delta$  6.70 ppm and  $\delta$  6.10 ppm in  $^1\text{H}$  NMR (Fig. 4b) and  $\delta$  130.57 ppm and  $\delta$  128.52 ppm in  $^{13}\text{C}$  NMR spectrum (Fig. S6b†). Also, the SEC overlay (Fig. 3b) reveals a decreased retention volume of VPOSS-cPS-ACPOSS relative to VPOSS-cPS-alkyne, which is consistent with the increased molecular weight and a larger hydrodynamic volume (SEC:  $M_{n, \text{SEC}} = 5.8 \text{ kg mol}^{-1}$ , PDI = 1.05, Table 1). Furthermore, MALDI-TOF mass spectrum in Fig. 5b provides a unimodal symmetric narrow molecular weight distribution with a typical  $m/z$  value of 5979.14 that corresponds well to the expected value for a 25-mer of VPOSS-cPS-ACPOSS ( $M_{\text{calcd}} = 5978.17 \text{ Da}$ , see Table 1). Therefore, it can be concluded that a cyclic polymer tethered with two different vinyl-functionalized POSS cages has been successfully synthesized.

The selective functionalization of individual POSS cage on PS macrocycle can be precisely achieved by using sequentially performed thiol-Michael and thiol-ene reactions based on the reactivity difference between acryloyl and vinyl groups. Under typical base-mediated thiol-Michael condition,<sup>51</sup> the first kind of functionality (*i.e.* 1H,1H,2H,2H-perfluoro-1-decanethiol) was introduced onto ACPOSS unit, with no side reactions to VPOSS cage or any byproducts from coupling of intermediates. This was supported by the presence of vinyl protons and carbons in  $^1\text{H}$  (Fig. 4c) and  $^{13}\text{C}$  NMR spectrum (Fig. S6c†), respectively. The increased overall molecular weight due to the incorporation of seven perfluorinated alkyl chains is also reflected by the clear shift in retention volume of VPOSS-cPS-FPOSS ( $M_{n, \text{SEC}} = 8.7 \text{ kg mol}^{-1}$ , PDI = 1.04, Table 1) compared with that of VPOSS-cPS-ACPOSS in SEC overlay (Fig. 3b). Finally, in the MALDI-TOF mass spectrum (Fig. 6), a single narrow molecular weight distribution can be clearly observed under the positive linear mode despite its relatively high molecular weight. Although monoisotopic resolution is not possible in this molecular weight range, the average molecular weights of the peaks match well with the calculated values (*e.g.*, for  $[\text{M}_{28}\cdot\text{Na}]^+$ , observed  $m/z$  9658.47 Da *vs.* calcd 9657.75 Da). Therefore, all the results obtained confirm the molecular structures and uniformity of the resulting product.

Radical-mediated thiol-ene reaction was then used to introduce a second functionality for the VPOSS unit by using a different thiol ligand such as 2-mercaptoacetic acid. Again, the successful surface modification was unambiguously supported by  $^1\text{H}$  NMR (Fig. 4d) and  $^{13}\text{C}$  NMR (Fig. S6d†). Furthermore, the SEC chromatogram of APOSS-cPS-FPOSS (Fig. 3b) exhibits



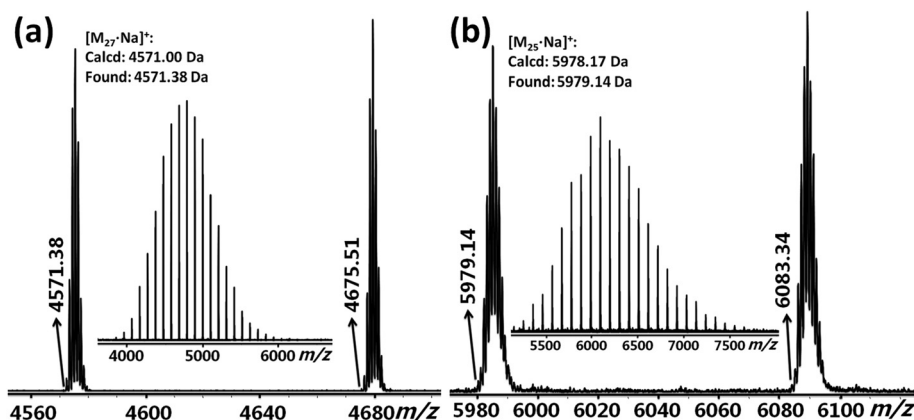


Fig. 5 MALDI-TOF mass spectra of (a) VPOSS-cPS-alkyne, and (b) VPOSS-cPS-ACPOSS. Both spectra were obtained in reflection mode with mono-isotopic resolution. The insets show the corresponding full spectra.

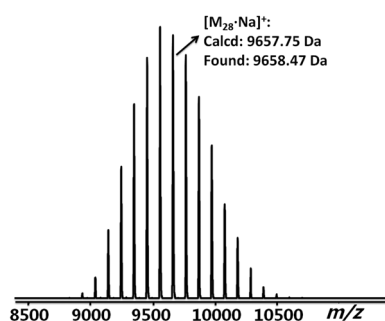


Fig. 6 MALDI-TOF mass spectrum of VPOSS-cPS-FPOSS, which was obtained in linear mode.

a monomodal, symmetric peak ( $M_{n, SEC} = 8.0 \text{ kg mol}^{-1}$ ,  $PDI = 1.07$ ). Similar to that of APOSS-cPS, there is a clear shift in higher retention volume compared to that of VPOSS-cPS-FPOSS after thiol-ene reaction, consistent with the decrease in overall hydrodynamic volume as a result of the change of the total amphiphilicity.<sup>47</sup> Notably, this product can be arguably regarded as a unique snowman-like molecular Janus particle (APOSS-FPOSS)<sup>21,31</sup> with a cyclic PS as the spacer. Strong phase segregation is anticipated among these three components, which could probably render novel self-assembled hierarchical structures and intriguing phase behaviors relative to simple molecular Janus particles such as APOSS-BPOSS.<sup>31</sup>

## Conclusions

In summary, we have successfully developed a multiple sequential “click” strategy based on the reactivity difference between DIBO and terminal alkyne groups, and between acryloxy groups and vinylsiloxanes. We have demonstrated that it is a general, robust, and efficient methodology by the facile synthesis of giant surfactants based on POSS(s) tethered with cyclic polymer. Notably, SPAAC reaction is found to be a powerful tool for macromolecular cyclization. This work not only offers new opportunities in macrocycle-based topological

polymer chemistry,<sup>33</sup> but also allows for the rational design and precision synthesis of a large variety of POSS-based giant surfactants with complex shapes and architectures for a systematic study of their structure–property relationships. Related work on elucidating the structure–property relationship and self-assembly behaviors of these unique materials are currently underway in our laboratory.

## Acknowledgements

This work was supported by the National Science Foundation (DMR-1408872) and the Joint-Hope Education Foundation. The work in Sichuan University was supported by a collaborative grant provided by the National Natural Science Foundation of China (51210005). Z. Zhang acknowledges the financial support from Jiangsu Overseas Research & Training Program for University Prominent Young and Middle-aged Teachers and Presidents and National Natural Science Foundation of China (21234005). We thank Ms. Kai Guo and Prof. Chrys Wesdemiotis for their help with the MALDI-TOF mass characterizations. We also acknowledge Mr Boyu Zhang at Tulane University for kind suggestions and helpful discussions.

## References

- 1 C. J. Hawker and K. L. Wooley, *Science*, 2005, **309**, 1200–1205.
- 2 R. K. Iha, K. L. Wooley, A. M. Nyström, D. J. Burked, M. J. Kade and C. J. Hawker, *Chem. Rev.*, 2009, **109**, 5620–5686.
- 3 K. Matyjaszewski, *Prog. Polym. Sci.*, 2005, **30**, 858–875.
- 4 D. Fournier, R. Hoogenboom and U. S. Schubert, *Chem. Soc. Rev.*, 2007, **36**, 1369–1380.
- 5 P. L. Golas and K. Matyjaszewski, *Chem. Soc. Rev.*, 2010, **39**, 1338–1354.
- 6 W. H. Binder and R. Sachsenhofer, *Macromol. Rapid Commun.*, 2007, **28**, 15–54.

- 7 B. S. Sumerlin and A. P. Vogt, *Macromolecules*, 2010, **43**, 1–13.
- 8 H. C. Kolb, M. G. Finn and K. B. Sharpless, *Angew. Chem., Int. Ed.*, 2001, **40**, 2004–2021.
- 9 Z. Wang, Y. Li, X.-H. Dong, X. Yu, K. Guo, H. Su, K. Yue, C. Wesdemiotis, S. Z. D. Cheng and W.-B. Zhang, *Chem. Sci.*, 2013, **4**, 1345–1352.
- 10 X. Feng, S. Zhu, K. Yue, H. Su, K. Guo, C. Wesdemiotis, W.-B. Zhang, S. Z. D. Cheng and Y. Li, *ACS Macro Lett.*, 2014, **3**, 900–905.
- 11 J.-F. Lutz, *Angew. Chem., Int. Ed.*, 2008, **47**, 2182–2184.
- 12 K. C. Nicolaou, S. A. Snyder, T. Montagnon and G. Vassilikogiannakis, *Angew. Chem., Int. Ed.*, 2002, **41**, 1668–1698.
- 13 H. Durmaz, A. Dag, O. Altintas, T. Erdogan, G. Hizal and U. Tunca, *Macromolecules*, 2007, **40**, 191–198.
- 14 A. B. Lowe, *Polym. Chem.*, 2010, **1**, 17–36.
- 15 Y. Li, W.-B. Zhang, J. E. Janoski, X. Li, X. Dong, C. Wesdemiotis, R. P. Quirk and S. Z. D. Cheng, *Macromolecules*, 2011, **44**, 3328–3337.
- 16 C. E. Hoyle and C. N. Bowman, *Angew. Chem., Int. Ed.*, 2010, **49**, 1540–1573.
- 17 M. J. Kade, D. J. Burke and C. J. Hawker, *J. Polym. Sci., Part A: Polym. Chem.*, 2010, **48**, 743–750.
- 18 K. L. Heredia, Z. P. Tolstyka and H. D. Maynard, *Macromolecules*, 2007, **40**, 4772–4779.
- 19 L. M. Campos, K. L. Killops, R. Sakai, J. M. J. Paulusse, D. Dameron, E. Drockenmüller, B. W. Messmore and C. J. Hawker, *Macromolecules*, 2008, **41**, 7063–7070.
- 20 C. A. Deforest, B. D. Polizzotti and K. S. Anseth, *Nat. Mater.*, 2009, **8**, 659–664.
- 21 W.-B. Zhang, X. Yu, C.-L. Wang, H.-J. Sun, I.-F. Hsieh, Y. Li, X.-H. Dong, K. Yue, R. M. Van Horn and S. Z. D. Cheng, *Macromolecules*, 2014, **47**, 1221–1239.
- 22 X. Yu, K. Yue, I.-F. Hsieh, Y. Li, X.-H. Dong, C. Liu, Y. Xin, H.-F. Wang, A.-C. Shi, G. R. Newkome, R.-M. Ho, E.-Q. Chen, W.-B. Zhang and S. Z. D. Cheng, *Proc. Natl. Acad. Sci. U. S. A.*, 2013, **110**, 10078–10083.
- 23 X. Yu, S. Zhong, X. Li, Y. Tu, S. Yang, R. M. Van Horn, C. Ni, D. J. Pochan, R. P. Quirk, C. Wesdemiotis, W.-B. Zhang and S. Z. D. Cheng, *J. Am. Chem. Soc.*, 2010, **132**, 16741–16744.
- 24 X. Yu, Y. Li, X.-H. Dong, K. Yue, Z. Lin, X. Feng, M. Huang, W.-B. Zhang and S. Z. D. Cheng, *J. Polym. Sci., Part B: Polym. Phys.*, 2014, **52**, 1309–1325.
- 25 S.-W. Kuo and F.-C. Chang, *Prog. Polym. Sci.*, 2011, **36**, 1649–1696.
- 26 M. F. Roll, M. Z. Asuncion, J. Kampf and R. M. Laine, *ACS Nano*, 2008, **2**, 320–326.
- 27 F. Wang, X. Lu and C. He, *J. Mater. Chem.*, 2011, **21**, 2775–2782.
- 28 D. B. Cordes, P. D. Lickiss and F. Rataboul, *Chem. Rev.*, 2010, **110**, 2081–2173.
- 29 K. Tanaka and Y. Chujo, *J. Mater. Chem.*, 2012, **22**, 1733–1746.
- 30 S. Fabritz, S. Hörner, O. Avrutina and H. Kolmar, *Org. Biomol. Chem.*, 2013, **11**, 2224–2236.
- 31 Y. Li, W.-B. Zhang, I.-F. Hsieh, G. Zhang, Y. Cao, X. Li, C. Wesdemiotis, B. Lotz, H. Xiong and S. Z. D. Cheng, *J. Am. Chem. Soc.*, 2011, **132**, 10712–10715.
- 32 B. A. Laurent and S. M. Grayson, *Chem. Soc. Rev.*, 2009, **38**, 2202–2213.
- 33 T. Yamamoto and Y. Tezuka, *Polym. Chem.*, 2011, **2**, 1930–1941.
- 34 C. W. Bielawski, D. Benitez and R. H. Grubbs, *Science*, 2002, **297**, 2041–2044.
- 35 H. R. Kricheldorf, *J. Polym. Sci., Part A: Polym. Chem.*, 2010, **48**, 251–284.
- 36 B. Chen, K. Jerger, J. M. J. Fréchet and F. C. Szoka Jr., *J. Controlled Release*, 2009, **140**, 203–209.
- 37 N. Nasongkha, B. Chen, N. Macaraeg, M. E. Fox, J. M. J. Fréchet and F. C. Szoka, *J. Am. Chem. Soc.*, 2009, **131**, 3842–3843.
- 38 D. E. Lonsdale and M. J. Monteiro, *Chem. Commun.*, 2010, **46**, 7945–7947.
- 39 B. A. Laurent and S. M. Grayson, *J. Am. Chem. Soc.*, 2006, **128**, 4238–4239.
- 40 B. Zhang, H. Zhang, Y. Li, J. N. Hoskins and S. M. Grayson, *ACS Macro Lett.*, 2013, **2**, 845–848.
- 41 W.-B. Zhang, F. Sun, D. A. Tirrell and F. H. Arnold, *J. Am. Chem. Soc.*, 2013, **135**, 13988–13997.
- 42 M. Glassner, J. P. Blinco and C. Barner-Kowollik, *Macromol. Rapid Commun.*, 2011, **32**, 724–728.
- 43 C. Schoene, J. O. Fierer, S. P. Bennett and M. Howarth, *Angew. Chem., Int. Ed.*, 2014, **53**, 6101–6104.
- 44 Z. Lin, P. Lu, X. Yu, W.-B. Zhang, M. Huang, K. Wu, K. Guo, C. Wesdemiotis, X. Zhu, Z. Zhang, K. Yue and S. Z. D. Cheng, *Macromolecules*, 2014, **47**, 4160–4168.
- 45 U. Tunca, *J. Polym. Sci., Part A: Polym. Chem.*, 2014, **52**, 3147–3165.
- 46 H. Su, Y. Li, K. Yue, Z. Wang, P. Lu, X. Feng, X.-H. Dong, S. Zhang, S. Z. D. Cheng and W.-B. Zhang, *Polym. Chem.*, 2014, **5**, 3697–3706.
- 47 H. Su, J. Zheng, Z. Wang, F. Lin, X. Feng, X.-H. Dong, M. L. Becker, S. Z. D. Cheng, W.-B. Zhang and Y. Li, *ACS Macro Lett.*, 2013, **2**, 645–650.
- 48 D. P. Nair, M. Podgórski, S. Chatani, T. Gong, W. Xi, C. R. Fenoli and C. N. Bowman, *Chem. Mater.*, 2014, **26**, 724–744.
- 49 S. Ates, Y. Y. Durmaz, L. Torun and Y. Yagci, *J. Macromol. Sci., Part A: pure appl. Chem.*, 2010, **47**, 809–815.
- 50 L. Li, C. He, W. He and C. Wu, *Macromolecules*, 2011, **44**, 8195–8206.
- 51 Y. Li, H. Su, X. Feng, Z. Wang, K. Guo, C. Wesdemiotis, Q. Fu, S. Z. D. Cheng and W.-B. Zhang, *Polym. Chem.*, 2014, **5**, 6151–6162.
- 52 Y. Li, X.-H. Dong, K. Guo, Z. Wang, Z. Chen, C. Wesdemiotis, R. P. Quirk, W.-B. Zhang and S. Z. D. Cheng, *ACS Macro Lett.*, 2012, **1**, 834–839.
- 53 J. Zheng, L. A. Smith Callahan, J. Hao, K. Guo, C. Wesdemiotis, R. A. Weiss and M. L. Becker, *ACS Macro Lett.*, 2012, **1**, 1071–1073.
- 54 Y. Li, Z. Wang, J. Zheng, H. Su, F. Lin, K. Guo, X. Feng, C. Wesdemiotis, M. L. Becker, S. Z. D. Cheng and W.-B. Zhang, *ACS Macro Lett.*, 2013, **2**, 1026–1032.

- 55 N. J. Agard, J. A. Prescher and C. R. Bertozzi, *J. Am. Chem. Soc.*, 2004, **126**, 15046–15047.
- 56 Y. Li, K. Guo, H. Su, X. Li, X. Feng, Z. Wang, W. Zhang, S. Zhu, C. Wesdemiotis, S. Z. D. Cheng and W.-B. Zhang, *Chem. Sci.*, 2014, **5**, 1046–1053.
- 57 P. G. Clark, E. N. Guidry, W. Y. Chan, W. E. Steinmetz and R. H. Grubbs, *J. Am. Chem. Soc.*, 2010, **132**, 3405–3412.
- 58 W.-B. Zhang, Y. Li, X. Li, X. Dong, X. Yu, C.-L. Wang, C. Wesdemiotis, R. P. Quirk and S. Z. D. Cheng, *Macromolecules*, 2011, **44**, 2589–2596.